Available on CMS information server

CMS NOTE 2006/123

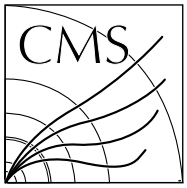

The Compact Muon Solenoid Experiment

CMS Note

Mailing address: CMS CERN, CH-1211 GENEVA 23, Switzerland

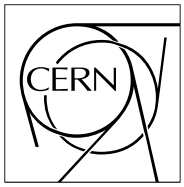

June 15, 2006

Study of Drell-Yan Dimuon Production with the CMS Detector

I. Belotelov, I. Golutvin, A. Lanyov, V. Palichik, E. Rogalev, M. Savina, S. Shmatov, V. Zykunov

Joint Institute for Nuclear Research, Dubna, Russia

D. Bourilkov

University of Florida, Gainesville, FL, USA

Abstract

The potential of the Compact Muon Solenoid (CMS) experiment to measure Drell-Yan muon pairs is studied. The efficiency of Level-1 and High Level Triggers to these events is investigated. Muon pairs can be explored by CMS with high precision up to very high invariant masses. Systematic errors are considered. The possibility of performing precise measurements of the forward-backward asymmetry is discussed.

1 Introduction

The Standard Model (SM) has been tested by the experiments at LEP, SLC and Tevatron with a high accuracy. In particular, the yield of lepton pairs produced mainly via Drell-Yan (DY) processes, i.e. quark-antiquark annihilation by exchange of photons or Z^0 bosons, is predicted by the SM with high precision. So far, the experimental data have shown no significant deviation from the SM predictions for the Drell-Yan continuum up to energy scales of several hundred GeV/c^2. The higher-order calculations of the lepton pair production cross section in the mass region $0.1 \div 0.8$ TeV$/c^2$ are indeed in good agreement with D0 and CDF data [1, 2].

However, many models predict various violations of the standard behaviour of SM spectra and, therefore, their testing in the new energy scale is one of the priority tasks of particle physics. The most direct way is to look for effects of new physics as individual resonances above the Drell-Yan continuum. This strategy is based on the predictions coming from various left-right symmetric models, extended gauge theories including grand unification theories, and models of composite gauge bosons [3, 4] or some extra dimension scenarios. In all these cases, new vector bosons, neutral Z$'$ or KK-excitations of Z^0 or RS1-graviton states, would appear at a mass scale of the order of one to several TeV$/c^2$ which can be studied at LHC [5, 6]. Another possibility is to search for deviations *in the invariant-mass differential cross section* in wide invariant mass regions, i.e. non-resonant signals, as, for example, in ADD model of extra-dimensional gravity [7] or fermion compositeness models [8, 9].

Other options for testing of SM are precise measurements of the *forward-backward asymmetry*, which is sensitive to new physics, as well as to one of the fundamental parameters of the Standard Model, the *electroweak mixing angle*, Θ^{lept}, which can be used, together with the top quark mass, to put constraints on the Higgs boson mass and new physics scenarios.

These studies can be performed with the Compact Muon Solenoid (CMS) which is able to trigger on hard muons and reconstruct them well for transverse momenta up to a few TeV/c. In this report, the analysis of the CMS potential to measure Drell-Yan dimuon pairs is presented. The Note is organized as follows: in Section 2 the tools used for signal and background simulation are described and preselected cross sections are given. Section 3 is devoted to the detector response and trigger-related issues of Drell-Yan studies. The detailed description of the CMS performances for off-line reconstruction of dimuon pairs is given in the same Section. The main results on Drell-Yan cross section are presented in Section 4, together with the possible sources of systematic errors, both theoretical and detector related.

The results presented here extend the studies for the LHC SM workshop (see [10] and references therein), using much more data, full and fast detector simulations and applying rigorous statistical procedures to determine the statistical and systematic uncertainties.

2 Event simulation and preselection

Simulation of the Drell-Yan events in proton-proton collisions at 14 TeV centre-of-mass energy is performed with the generator package CMKIN [11] interfaced to the PYTHIA generator version 6.217 [12] using the CTEQ5L parton distribution functions [13]. The possible contributions from higher-order terms in the dimuon production cross section are taken into account by using a K factor of 1.3. Eleven samples of 10 000 events each with different cut-off values on the dimuon invariant mass are generated: $M_{inv} \geq$0.2, 0.5, 1, 1.5, 2, 2.5, 3, 3.5, 4, 4.5, 5 TeV$/c^2$. The total production cross sections are given in Table 1.

Table 1: Leading-order cross sections of Drell-Yan production in fb for different cut-off values on the dimuon mass. The CTEQ5L parton distributions are used. The cross section for preselected events is also given. The preselection cuts are $\eta_{\mu_1\mu_2} \leq 2.5$, $p_T \geq 7$ GeV/c.

$M_{\mu^+\mu^-}$, TeV/c^2	≥ 1.0	≥ 1.5	≥ 2.0	≥ 2.5	≥ 3.0	≥ 4.0
Drell-Yan	6.61	1.04	$2.39 \cdot 10^{-1}$	$6.53 \cdot 10^{-2}$	$1.97 \cdot 10^{-2}$	$2.09 \cdot 10^{-3}$
Preselected Drell-Yan	5.77	$9.53 \cdot 10^{-1}$	$2.24 \cdot 10^{-1}$	$6.14 \cdot 10^{-2}$	$1.87 \cdot 10^{-2}$	$2.00 \cdot 10^{-3}$

Only events with at least two muons in the pseudorapidity range $|\eta| \leq 2.5$, with transverse momentum $p_T \geq 7$ GeV/c for each muon are preselected. No cuts on isolation of muons are made at the preselection stage. The total efficiency for dimuon preselection, ε, is about 87 % for a mass of 1 TeV/c^2 and 96 % for a mass of 5 TeV/c^2. The preselected cross sections of Drell-Yan production are given in Table 1.

3 Detector response, trigger and off-line reconstruction

3.1 Detector response and digitization

To simulate the detector geometry, materials and particle propagation inside the detector, the GEANT4-based OSCAR package [14] is used. The digitization and reconstruction is performed with the CMS object-oriented reconstruction package ORCA [15].

3.2 Trigger selection

The trigger simulation is realized on the basis of the ORCA package using the on-line reconstruction algorithm. We require for each event the trigger condition for "double muon" or "single muon". This means that at least one muon candidate is within pseudorapidity region $|\eta| \leq 2.1$.

The Level-1 trigger performs a first selection over the events. It passes only events containing two muons with a transverse momentum greater than 3 GeV/c or one inclusive muon with a momentum greater than 14 GeV/c [16]. The efficiency of the Level-1 trigger for the analyzed samples is 99 %.

All events accepted by Level-1 Trigger are submitted to the High-Level Trigger (HLT). The HLT algorithms [16] reconstruct events in two stages – first of all, the Level-2 algorithm using information only from muon chambers is applied to re-evaluate the p_T of muons coming from Level-1. At the next step, on Level-3 the tracker hits are added to the muon tracks to refine finally the p_T measurements. The additional cuts on tracker isolation of muon track have been applied at the HLT level. The thresholds used at the muon HLT selection are 7 GeV/c for the HLT double muon trigger and 19 GeV/c for the HLT single muon trigger [16]. The total efficiency of triggering including reconstruction and trigger selection efficiency is 98 %. There is a significant decrease in trigger efficiency after applying of the Level-2 calorimeter isolation cuts (down by 15 %). The Level-3 tracker isolation practically does not affect the trigger efficiency. The reason for such a drop is related with the muon shower expansion with energy due to electromagnetic radiation and interactions of muons. The additional cuts on calorimeter and tracker isolation of muon tracks are not applied in this analysis, the ORCA implementation of trigger algorithm without these cuts has been used.

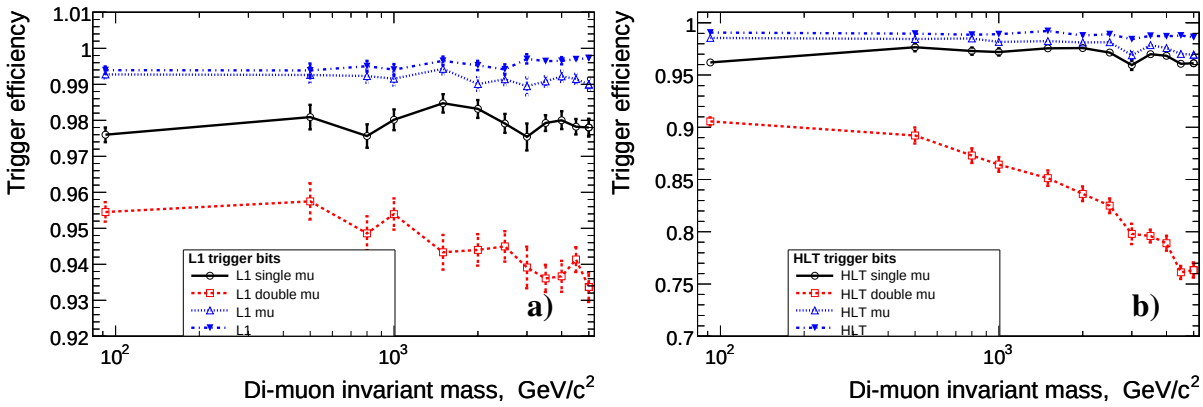

Figure 1: Dimuon trigger efficiency as function of cut for invariant mass. (a) L1 efficiency, (b) HLT efficiency.

The feasibility and overall performance of the muon trigger for Drell-Yan processes are summarized in Fig. 1. The total efficiency of triggering including reconstruction and trigger selection efficiency is 98 % at 1 TeV/c^2. The mass resolution of reconstructed dimuon pairs after HLT is better than 6 % for a perfectly aligned and calibrated detector referred to as an ideal detector.

3.3 Off-line reconstruction

The off-line reconstruction algorithm Global Muon Reconstructor (GMR) [17] of ORCA package is applied only to events which have passed trigger selection. At the off-line level two muons inside the CMS acceptance $|\eta| \leq 2.4$ and at least one muon inside the trigger acceptance $|\eta| \leq 2.1$ are required. No isolation criteria for off-line reconstructed tracks were used.

The off-line reconstructed invariant-mass spectra for the Drell-Yan events with M_{inv} cut-off 500 GeV/c^2, 1 TeV/c^2,

3 TeV/c^2 and 5 TeV/c^2 are given in Figure 2. The histograms for generated events are also presented. The invariant masses resolution spectra are given in Figure 3. The off-line reconstruction efficiency for samples with SM Drell-Yan events is about 98 $\div$ 94 % for masses 0.2 TeV/c^2 $\div$ 5 TeV/c^2. The *Long Term* misalignment scenario is considered. Note, there are two scenarios of misalignment of the Muon detector and Tracker for usage in the CMS studies: *First Data* scenario corresponding to the initial period of alignment (up to approximately 1 fb^{-1} integrated luminosity), and *Long Term* scenario corresponding the nominal CMS operation (see details in [18]).

The overall efficiency of the full reconstruction procedure taking into account trigger and off-line reconstruction inefficiency is 97 $\div$ 93 % for a mass range 0.2 TeV/c^2 $\div$ 5 TeV/c^2. (Figure 4, left). In the case of an ideal detector the mass resolution smearing for fully-reconstructed events is in the 1.8 $\div$ 6 % range for the mass interval 0.2 $\div$ 5 TeV/c^2 (Figure 4, right). The charge mis-identification probability is not taken into account for these curves. The percentage of mis-assigned charge for muons with p_T = 1000 GeV/c^2 is less than 2.0% for $|\eta| \leq 2.1$.

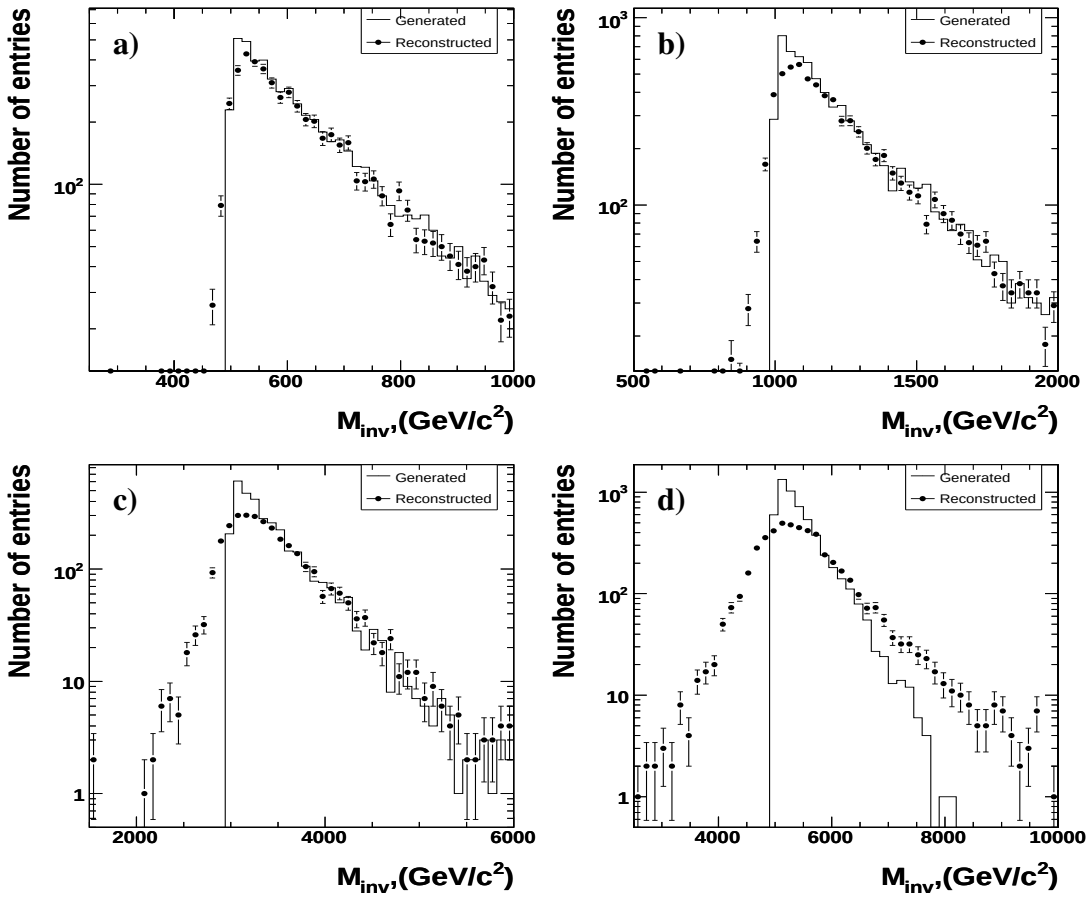

Figure 2: The reconstructed and generated invariant mass spectra for the DY events with M_{inv} cut-off (a) 500 GeV/c^2, (b) 1 TeV/c^2, (c) 3 TeV/c^2 and (d) 5 TeV/c^2 (left-to-right and top-to-bottom). The *Long Term* misalignment scenario is considered.

Examples of the reconstructed and generated kinematic distributions of muons for DY events with $M_{inv} \geq 0.5$, 1.0, 3.0 and 5.0 TeV/c^2 are shown in Figs. 5 and 6. One observes that both the reconstructed polar and azimuthal angle are in a good agreement with the generated ones. The distribution of reconstructed transverse momentum is somewhat broader than the generated distribution, with some small feed-up of the reconstructed dimuons to the high-mass region due to the finite momentum resolution.

In addition, we used a cross-check independent samples (71000 events in total) for a first tune of the parametrized efficiency for TeV muons utilized in the fast simulation and reconstruction package FAMOS [19]. After tuning, the FAMOS results on dimuon efficiency are in good agreement with the full simulation and reconstruction.

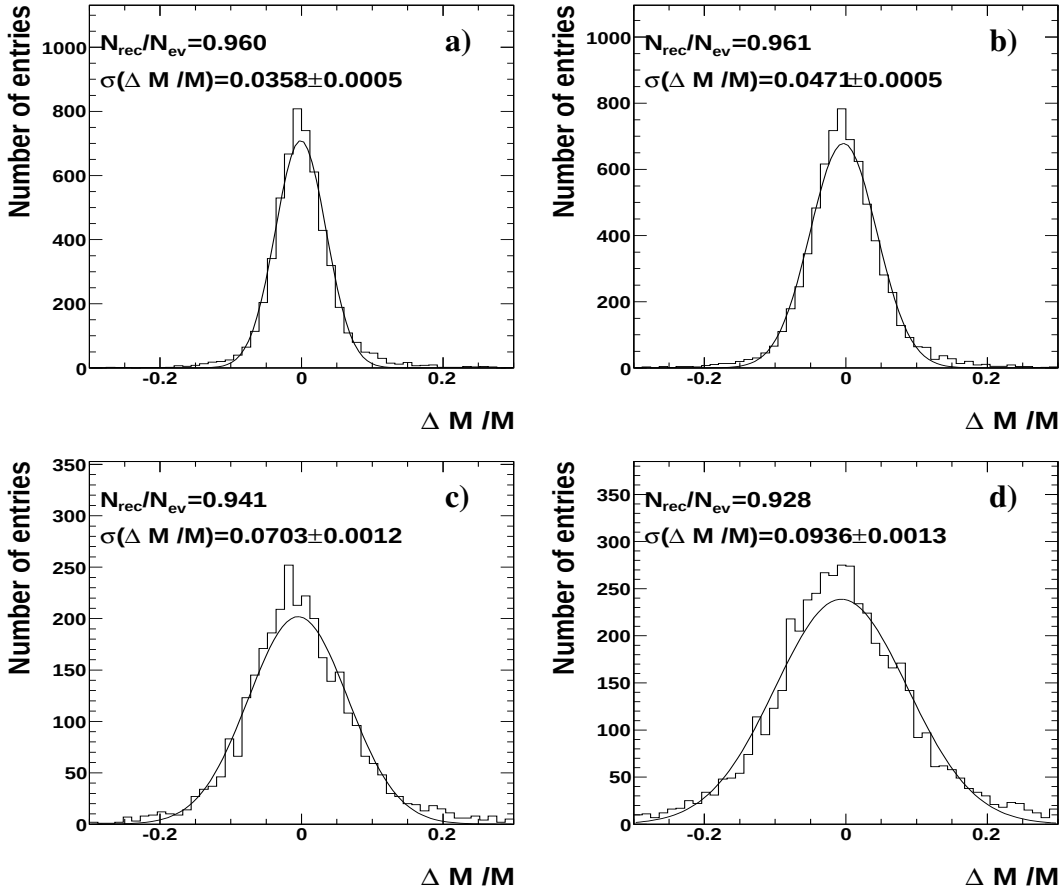

Figure 3: The invariant mass resolution spectra for the DY events with M_{inv} cut-off (a) 500 GeV/c^2, (b) 1 TeV/c^2, (c) 3 TeV/c^2 and (d) 5 TeV/c^2 (left-to-right and top-to-bottom). The *Long Term* misalignment scenario is considered.

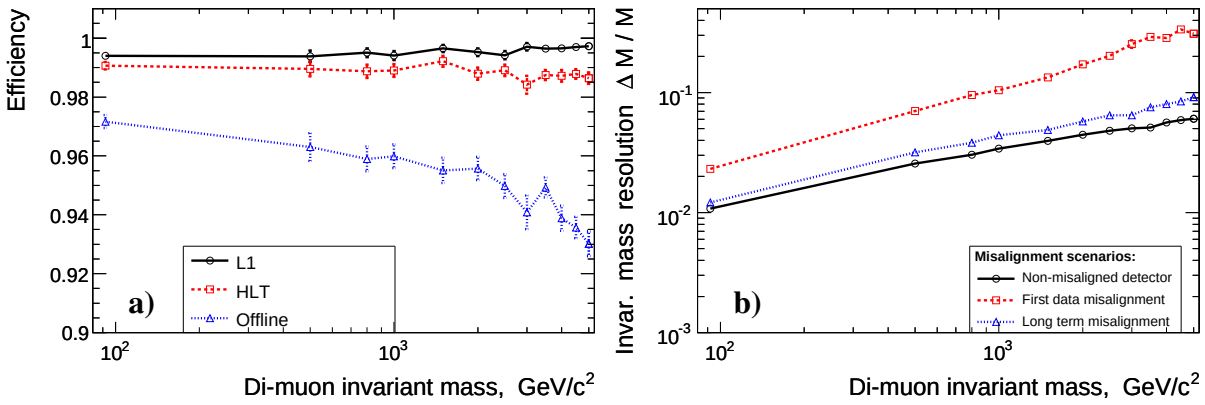

Figure 4: Dimuon trigger and reconstruction efficiency (a) and invariant mass resolution (b) as function of the invariant mass cut.

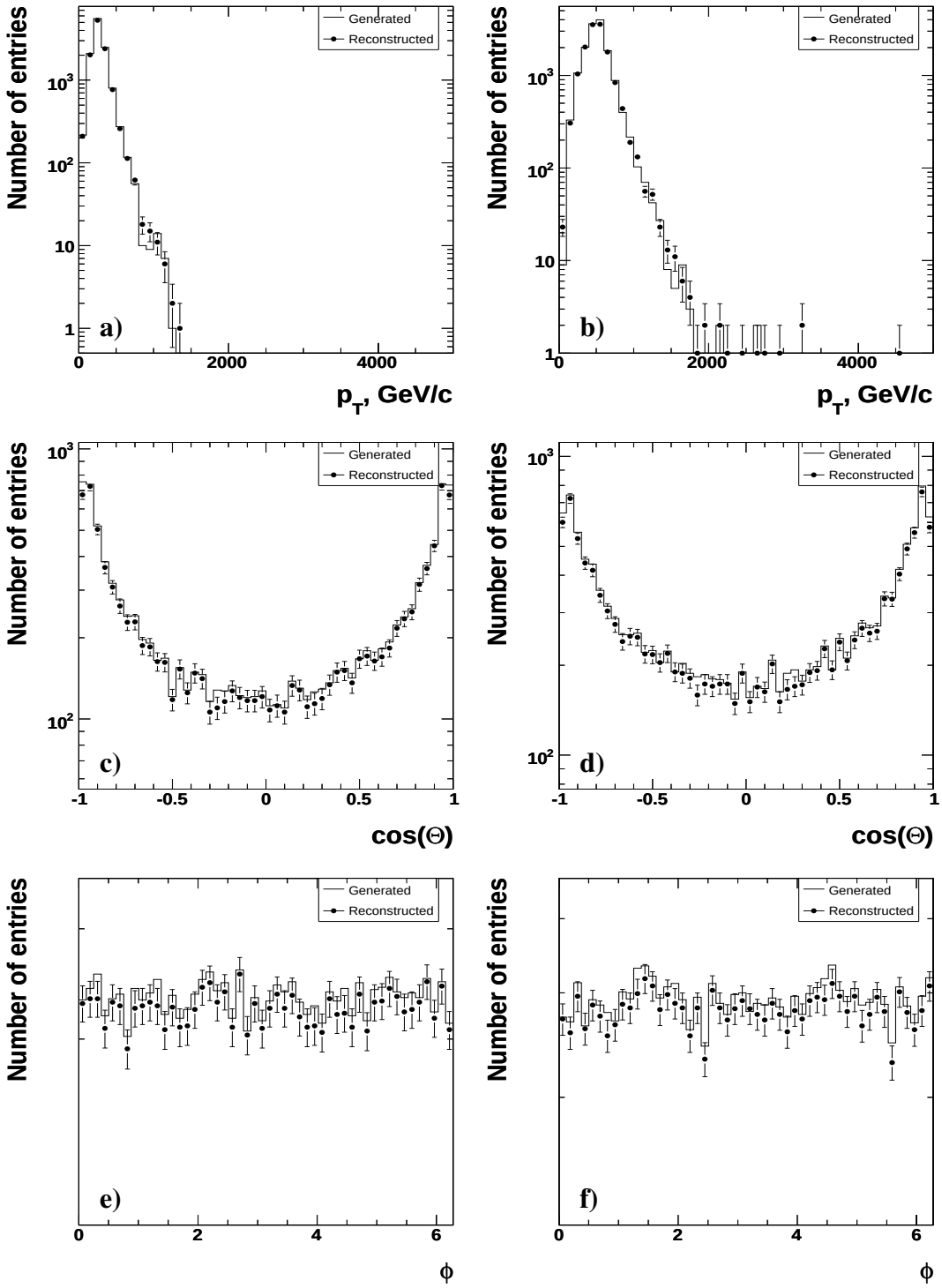

Figure 5: The reconstructed and generated (a,b) p_T, (c,d) $cos\theta$, and (f,e) ϕ spectra for the DY events with M_{inv} cut-off 500 GeV/c^2(left side) and 1 TeV/c^2 (right side). The *Long Term* misalignment scenario is considered.

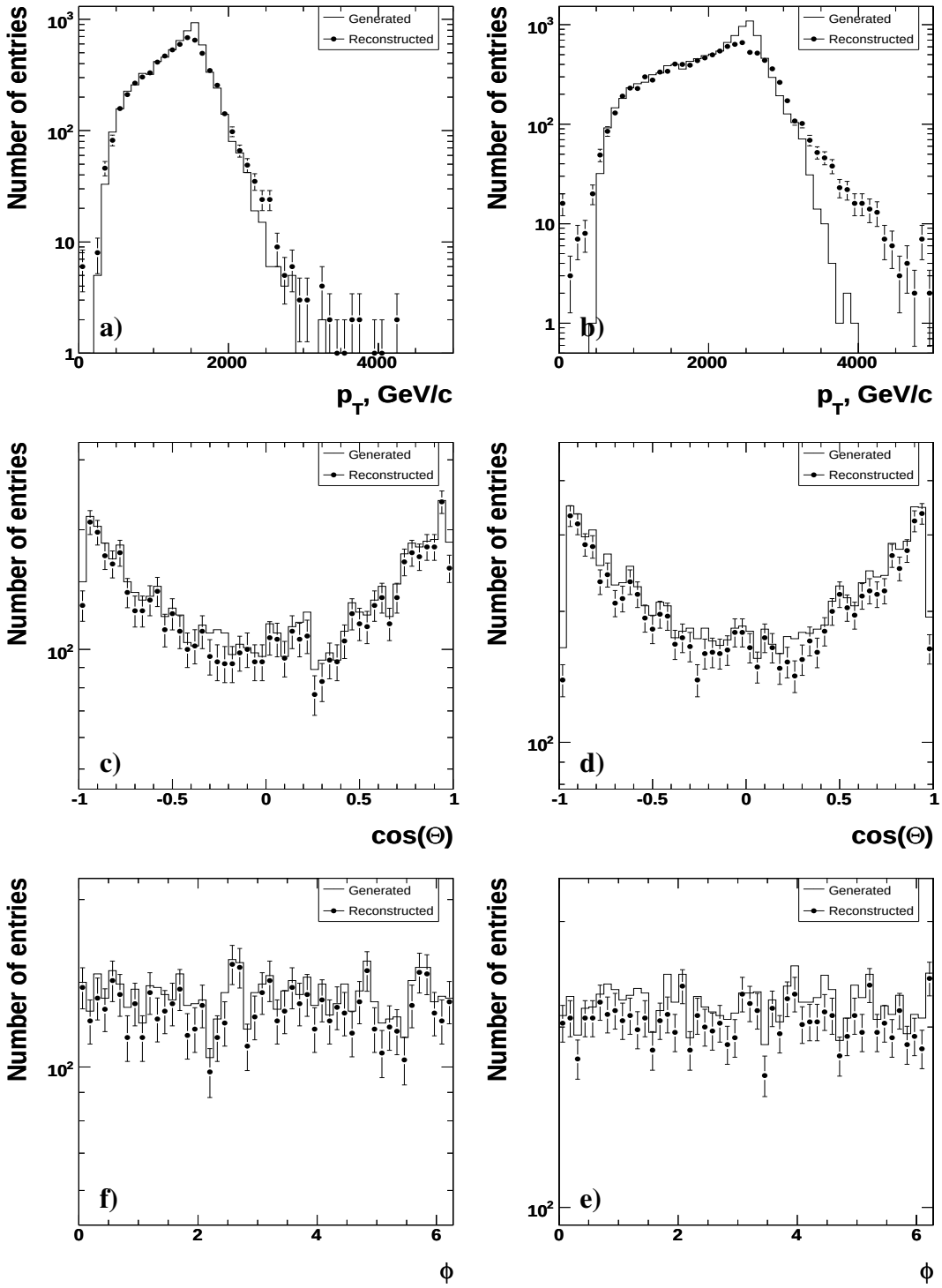

Figure 6: The reconstructed and generated (a,b) p_T, (c,d) $cos\theta$, and (e,f) ϕ spectra for the DY events with M_{inv} cut-off 3 TeV/c^2 (left side) and 5 TeV/c^2 (right side). The *Long Term* misalignment scenario is considered.

4 Results

At hadron colliders the parton cross sections are folded with the parton density functions (PDF): $pp \rightarrow l_1 l_2 + X$

$$\frac{d^2\sigma}{dM_{ll}dy}[pp \rightarrow l_1 l_2 + X] \sim \sum_{ij} \left(f_{i/p}(x_1) f_{j/p}(x_2) + (i \leftrightarrow j) \right) \hat{\sigma} \tag{1}$$

where $\hat{\sigma}$ is cross section for the partonic subprocess $ij \rightarrow l_1 l_2$, $M_{ll} = \sqrt{\tau s} = \sqrt{\hat{s}}$ the mass of the lepton-pair system, y the rapidity of the lepton pair, $x_1 = \sqrt{\tau} e^{y}$, $x_2 = \sqrt{\tau} e^{-y}$ the parton momentum fractions, and $f_{i/p(\bar{p})}(x_i)$ the probability to find a parton i with momentum fraction x_i in the proton.

The cross sections of Drell-Yan production for the CMS runs are shown in Table 2. The statistical errors for 1, 10 and 100 fb^{-1} runs and the uncertainty due the finite mass resolution, referred to as detector smearing are given in Table 2.

Table 2: Relative errors of the Drell-Yan muon pairs cross section measurements.

$M_{\mu^+\mu^-}$	Cross section fb	Detector smearing	Statistical 1 fb^{-1}	Statistical 10 fb^{-1}	Statistical 100 fb^{-1}
$\geq$ 200 GeV/c^2	$2.76 \cdot 10^3$	$8 \cdot 10^{-4}$	0.025	0.008	0.0026
$\geq$ 500 GeV/c^2	$1.07 \cdot 10^2$	0.0014	0.11	0.035	0.011
$\geq$ 1000 GeV/c^2	6.61	0.0049	0.37	0.11	0.037
$\geq$ 2000 GeV/c^2	$2.4 \cdot 10^{-1}$	0.017		0.56	0.18
$\geq$ 3000 GeV/c^2	$1.9 \cdot 10^{-2}$	0.029			0.64

To test the helicity structure of the exchanged particles and discriminate between different new physics scenarios, the leptonic forward-backward asymmetry can be used [20, 21, 22]. It can be defined through the differential cross section as a coefficient which is odd in $\cos\theta^*$:

$$\frac{d\sigma}{d(\cos\theta^*)} = c \left[\frac{3}{2(3+b)} \left(1 + b\, \cos^2\theta^*\right) + A_{FB}\, \cos\theta^* \right] \tag{2}$$

where θ^* is the angle between the outgoing negative lepton and the quark q in the dimuon rest frame.
Another definition can be

$$\sigma_{F\pm B}(y, M) = \left[\int_0^1 \pm \int_{-1}^0 \right] \sigma_{ll} d(\cos\theta^*) \tag{3}$$

$$A_{FB}(y, M) = \frac{\sigma_{F-B}(y, M)}{\sigma_{F+B}(y, M)}. \tag{4}$$

where the forward and backward directions are defined as $\cos\theta^* > 0$ and $\cos\theta^* < 0$, respectively.

Table 3: x_1 and x_2 for different masses and rapidities.

y	0	2	4
M = 91.2 GeV/c^2			
x_1	0.0065	0.0481	0.3557
x_2	0.0065	0.0009	0.0001
M = 200 GeV/c^2			
x_1	0.0143	0.1056	0.7800
x_2	0.0143	0.0019	0.0003
M = 1000 GeV/c^2			
x_1	0.0714	0.5278	-
x_2	0.0714	0.0097	-

The total cross section and the forward-backward asymmetry are function of observables which are well measured experimentally for e^+e^- and $\mu^+\mu^-$: the invariant mass and the rapidity of the final state lepton-pair. This allows to reconstruct the center-of-mass energy of the initial partons, even if their flavors are unknown. For a ($x_1 \geq x_2$) pair of partons we have 4 combinations of *up*- or *down*-type quarks initiating the interaction: $u\bar{u}, \bar{u}u, d\bar{d}, \bar{d}d$. In

pp collisions the antiquarks come always from the sea and the quarks can have valence or sea origin. The x-range probed depends on the mass and rapidity of the lepton-pair as shown in Table 3. Going to higher rapidities increases the difference between x_1 and x_2 and hence the probability that the first quark is a valence one. This allows a measurement of the forward-backward asymmetry even for the symmetric initial pp state.

4.1 Systematic uncertainties

For correct measurements and final data analysis it is necessary to keep under control all possible sources of errors and systematic uncertainties coming from different sources. These systematic uncertainties can be related to the accuracy of theoretical calculations, accuracy of phenomenological determination of PDF's and the experimental uncertainties – detector resolution, quality of fits etc.

4.1.1 Experimental Systematic Effects

The main systematic effects in the cross section measurement come from the total muon inefficiency and momentum resolution. The latter is very important at high mass values as smearing from lower masses from the steeply falling Drell-Yan spectrum can contaminate the high mass measurements, especially if the tails of the momentum resolution are not under control. The main sources of systematic uncertainties on the momentum resolution come from the alignment of the muon chambers and the central tracker, both at start-up and high luminosity.

Trigger efficiency: Taking into account the trigger efficiency changes from 98.5 % to 97% for masses from 0.2 to 5 TeV/c^2, very conservatively we assign half of this difference, i.e. 0.75 %, as a systematic uncertainty at the beginning of data taking.

Mass resolution: The modification of the measured cross section due to the smearing of the dimuon mass according to the expected mass resolution in the detector does not exceed 2.9% which is the value for masses above 3 TeV/c^2 (Table 2).

Misalignment: The misalignment does not affect the efficiency of dimuon reconstruction for any masses. The updated results from Reference [18] are presented in Figure 7. The effect of misalignment on the mass resolution is larger and varies from 1.1% up to 2.3% (1.3%) for the *First Data* (*Long Term*) scenarios at the Z^0 and from 5% up to 25% (6%) for 3 TeV/c^2 (Fig 4 (right)).

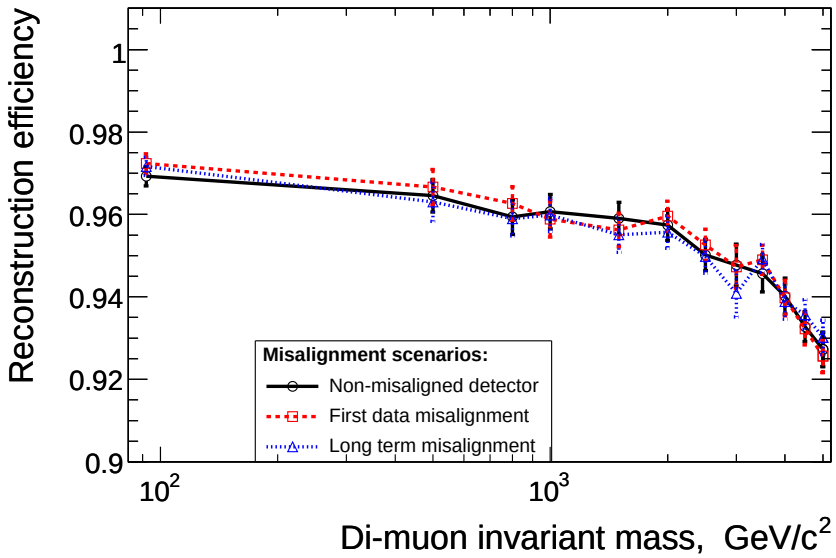

Figure 7: Dimuon reconstruction efficiency as function of the invariant mass cut. Different misalignment scenarios are considered.

Luminosity: An important ingredient in the cross section measurement is the precise determination of the luminosity. A promising possibility is to go directly to the parton luminosity [23] by using the $W^{\pm}$ (Z) production of single (pair) leptons:

- constraint the p.d.f.
- measure directly the parton-parton luminosity

New estimates show that in this way the systematic error on $\sigma_{DY}^{high\ Q^2}$ *relative* to σ_Z can be reduced to $\sim$ 5-12 % [9].

4.1.2 Theoretical Systematic Effects

K-factor (QCD corrections): For a full-scale analysis of experimental data in a hadron collision, it is necessary to fully understand and control higher order QCD corrections.

The possible theoretical ambiguity in such studies is induced by incomplete accounting of QCD contributions and electroweak higher order quantum corrections to the considered processes. The leading order corrections are often taken into account with K-factor of 1.3 [1)]. It is expected that the total value of additional NNLO contributions does not exceed 8 % .

Electroweak Radiative Corrections: The comparison data with theory, study of acceptance corrections for precise measurement of σ and A_{FB} at large centre-of-mass energies $\hat{s}$ requires good knowledge of the different types of genuine electroweak (EW) radiative corrections to the DY process: vertex, propagator, EW boxes. A complete one-loop parton cross section calculation has been included in [10] and confirmed in [25]. The size of the EW radiative corrections after folding with the parton distribution functions and the expected experimental precision of the cross section measurement are compared in Figure 8. The calculation [26] of the weak radiative corrections to the Drell-Yan processes due to additional heavy bosons contributions shows that these corrections are about 2.9 $\div$ 9.7 % for mass region 0.2 $\div$ 5 TeV/c^2. The effect of the PDFs on the weak radiative corrections in this very high mass regime is not essential. For example, the size of corrections for 1 TeV/c^2 pairs is 0.068 and 0.069 for CTEQ6 and MRST 2004-QED sets respectively.

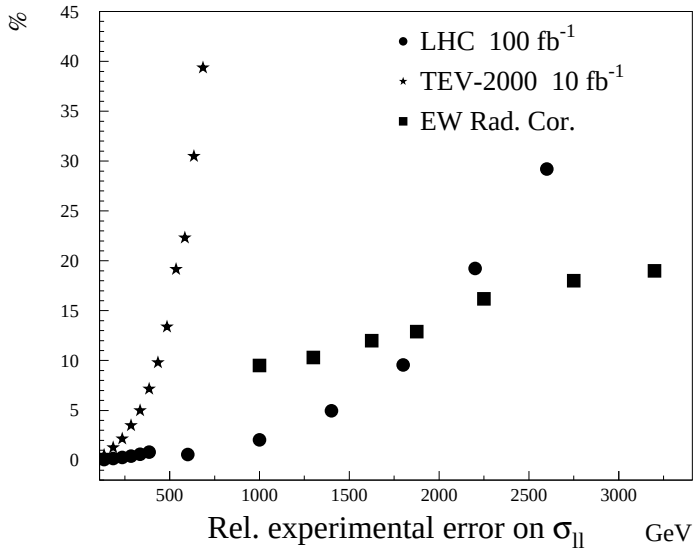

Figure 8: Size of the EW radiative corrections and the expected relative experimental precision on the cross section measurement for e^+e^- and $\mu^+\mu^-$ in CMS (for an ideal detector) in % as a function of the dilepton mass.

[1)] Calculations by M.Schmitt with the program PHOZPRMS [24].

PDF (internal errors and uncertainties of choice of PDF): The phenomenological origin of PDF gives one additional systematic error. First of all, estimates of cross section obtained by using different sets of structure functions do not give exactly the same values. The results vary within ± 7 % for $M_{ll} \geq 1$ TeV/c^2.

In addition, there are uncertainties within the bounds of the same set (so called *internal* uncertainties) coming from the accuracy of the global analysis of experimental data and from experimental measurement errors. The recently developed PDF's building technique goes beyond the "standard" paradigm of extracting one "best fit". The last versions of PDF's contain sets of various alternative fits obtained by varying specific degrees of freedom for this PDF [27, 28, 29]. Applying standard statistical methods, it allows to analyze *internal* uncertainties comprehensively. These uncertainties are especially large for very large values of x (or Q^2) and in the small-x region. For instance, the uncertainty bands for CTEQ6M set of PDF's stay within the limits of 2.6 % and 6 % for u- and d-quarks respectively in the range of x values from $10^{-3} \div 10^{-4}$ up to 0.3 at Q^2 = 10 GeV^2, and then they rapidly grow for large x and can reach ~ 50 % at $x = 0.6 \div 0.7$ [30].

Naturally, the ambiguity in theoretical calculations of Drell-Yan cross section due to *internal* uncertainties of PDF's might also be very large. Thus, for invariant masses available to date for the Tevatron ($\sim$ 0.8 TeV/c^2) this uncertainty is of the order of the theoretical one which is not larger than ± 6 %, but the calculation accuracy strongly decreases for large values of invariant masses, down to $\sim 10 \div 15$ % for 3 TeV/c^2 (Fig. 9). Around this region (near 2.5 TeV/c^2) the error coming from PDF's is of the order of the statistical one expected for integrated luminosity of 300 fb^{-1} (about three years of LHC operations at the high-luminosity regime).

The major ambiguity in Drell-Yan calculations comes from PDF uncertainties. One expects that the LHC will extend the ranges in x and Q^2 available for analysis, and together with data from both working machines, the Tevatron and HERA, will determine parton distribution functions more precisely. Moreover, definite progress is also possible from the theoretical side due to precise taking into account both of higher twist terms and nonperturbative QCD effects [30].

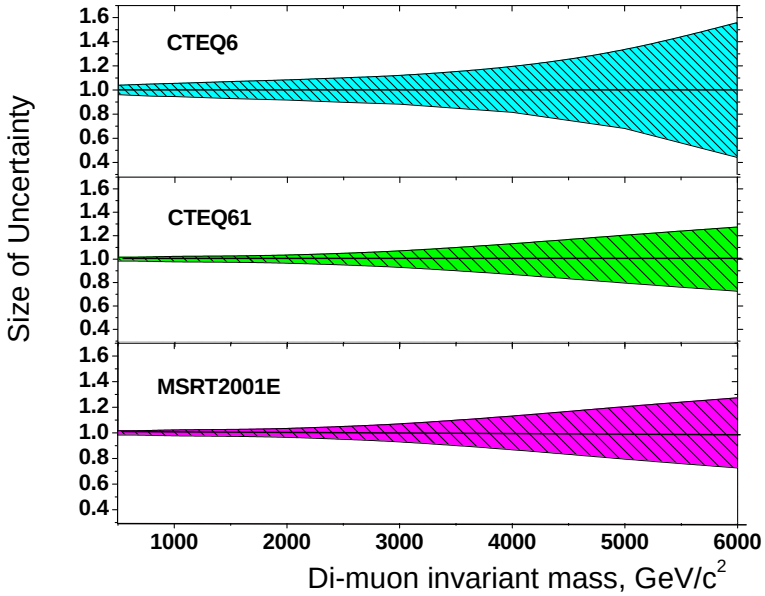

Figure 9: PDF's uncertainties in Drell-Yan production as function of the dimuon invariant mass cut.

PDF-dependence of the acceptance efficiency: Variation of the PDF sets (CTEQ5L, CTEQ6L, MRST2001E) leads to changes in the acceptance efficiency up to 0.5 %. The ambiguity in the acceptance efficiency due to internal PDF's uncertainties is larger, but less than 1.4 % for any mass region.

Hard processes scale: In dependence on the definition of Q^2 scale the Drell Yan cross section varies within a few percent for low invariant mass region up to 13 % for large invariant-mass region, for the CTEQ6 PDF set [30], see Figure 10 where the theoretical uncertainties (PDF and hard processes scale) are given in comparison with detector errors. These values were calculated following the method described in [31].

Background: The backgrounds considered are vector boson pair production ZZ, WZ, WW, $t\bar{t}$ production etc. The simulation and preselection of background events is done using CMKIN [11] with the same cuts as for the signal above. In the SM the expected leading-order cross section of these events is negligible in comparison with the Drell-Yan one (Table 4).

Table 4: Leading-order cross sections of pre-selected di-bosons (ZZ, ZW, WW) and $t\bar{t}$ events in fb for different cut-off values on the dimuon mass. The CTEQ5L parton distributions are used.

$M_{\mu^+\mu^-}$, TeV/c^2	≥ 1.0	≥ 1.5	≥ 2.0	≥ 2.5	≥ 3.0	≥ 4.0
Di-bosons, fb	$2.59 \cdot 10^{-4}$	$1.51 \cdot 10^{-4}$	$5.6 \cdot 10^{-5}$	$2.26 \cdot 10^{-5}$	$9.06 \cdot 10^{-6}$	$1.66 \cdot 10^{-6}$
$t\bar{t}$, fb	$2.88 \cdot 10^{-4}$	$2.58 \cdot 10^{-4}$	$1.55 \cdot 10^{-4}$	$7.02 \cdot 10^{-5}$	$2.93 \cdot 10^{-5}$	$3.65 \cdot 10^{-6}$

The $\tau\tau$ background (from τ decaying to μ and neutrinos) is 0.8 % at the Z pole and 0.7 % for masses above 1 TeV/c^2. The background from Drell-Yan production of $q\bar{q}$ pairs (mostly semileptonic b or c decays) is 0.3 % at the Z pole without applying any isolation cuts and below 0.1 % for masses above 1 TeV/c^2.

The other background sources are negligible. If the need arises they can be further suppressed by acoplanarity and isolation cuts in the tracker.

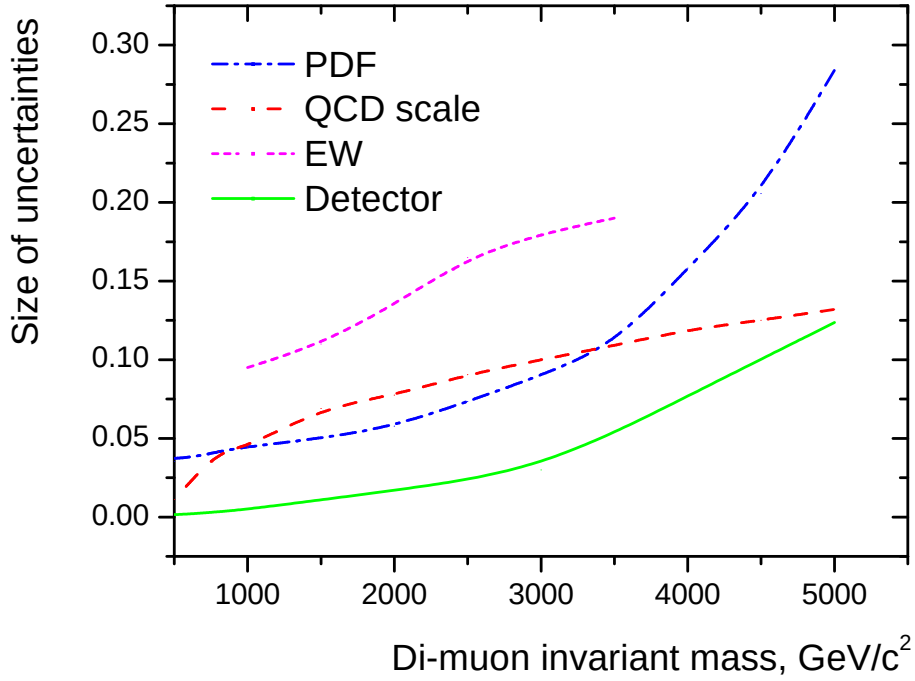

Figure 10: Size of the EW corrections and the cross section uncertainties from PDFs, hard process scale and detector performances as a function of the dimuon invariant mass cut.

The comparison of values of possible uncertainties is given in Figure 10.

4.2 Prospects on the measurement of the forward-backward asymmetry

To measure the forward-backward asymmetry we need the original quark and anti-quark directions of the initiating partons, but these are not known in the case of pp experiments, where the initial state is symmetric. In Ref. [32, 33] it is shown that it is possible to approximate the quark direction with the boost direction of the dimuon system with respect to the beam axis. This is due to the fact that the valence quarks have on average larger momentum than the sea antiquarks, and therefore the dimuon boost direction approximates the quark direction. The most unambiguous tagging occurs for large dimuon rapidity.

The approximation of the original quark direction for pp collisions leads to a flattening out of the original asymmetry (≈ 0.61 for Drell-Yan events) by a factor of almost 2. However, using multi-dimensional fits [5] or reweighting techniques depending on the mistag and acceptance which are under development, we can measure the original

asymmetry.

The accuracy of asymmetry measurements depends on:

- statistical uncertainty which grows with rising mass cut value, as the number of events for integrated luminosity of e.g. $\int \mathcal{L}\, dt = 100\,\text{fb}^{-1}$ decreases with mass and the accuracy is order to 7 % for masses above 1 TeV/c^2.
- systematic uncertainty from the variation of the mistag probabilities for various PDF sets, typically below 7 %.

We expect the systematic uncertainty to dominate the statistical one for integrated luminosity of $\int \mathcal{L}\, dt = 100\,\text{fb}^{-1}$ and dimuon masses around 500 GeV/c^2, while the statistical one to be more important for dimuon mass cuts above 1000 GeV/c^2. A CMS note on A_{FB} asymmetry is under preparation.

Summary

In this note we have investigated in detail the potential of the CMS experiment to measure the cross section and the forward-backward asymmetry for dimuon pairs up to the highest masses that will be accessible at the LHC, and to test the Standard Model up to very high momentum transfers in a new and unexplored energy range. The total relative systematic uncertainties for the cross section of Drell-Yan pair production are estimated. It is shown that systematic uncertainties from theory are larger than detector effects due to misalignment, acceptance uncertainties etc. The statistical errors dominate for invariant mass larger than 2 TeV/c^2 even for 100 fb^{-1}. For high invariant mass regions the accuracy of the forward-backward asymmetry is limited by the number of events (e.g. 7 % for masses above 1 TeV/c^2 and 100 fb^{-1}) and systematic effects (below 7 %) .

Acknowledgments

We would like to thank Albert De Roeck and Joachim Mnich for many helpful conversations and communications, and all members of Muon PRS Group for their help and discussion of reconstruction and analysis issues, especially to Ugo Gasparini, Norbert Neumeister and Darin Acosta. We are also very thankful to Andrei Arbuzov and Dmitry Bardin for their contributions and discussions of EW corrections, and to Robert Cousins and Jason Mumford for discussion of the forward-backward asymmetry. I. Belotelov acknowledges the financial support provided by the INTAS program.

References

[1] D0 Collaboration, B. Abbott *et al.*, Phys. Rev. Lett. **82** (1999) 4769;
D0 Collaboration, V.M. Abazov *et al.*, Phys. Rev. Lett. **95** (2005) 091801.

[2] CDF Collaboration, F. Abe *et al.*, Phys. Lett. **B 391** (1997) 221;
CDF Collaboration, D. Acosta *et al.*, Phys. Rev. **D71** (2005) 052002.

[3] M. Cvetič and S. Godfrey, Summary of the Working Subgroup on Extra Gauge Bosons of the PDF long-range planning study to *Electro-weak Symmetry Breaking and Beyond Standard Model*, eds. T. Barklow *et al.*, World Scientific, 1995; hep-ph/9504216;
T.G. Rizzo, *Proceedings of the 1996 DPF/DPB Summer Study on New Directions for High Energy Physics-Snowmass96*, Snowmass, CO, 25 June - 12 July, 1996.

[4] J.L. Hewett and T.G. Rizzo, Phys. Rept. **183** (1989) 193.

[5] R. Cousins, J. Mumford, and V. Valuev, "Detection of Z' Gauge Bosons in the Dimuon Decay Mode in CMS", CMS NOTE-2005/002; CMS NOTE-2006/062.

[6] I. Belotelov *et al.*, "Search for Randall-Sundrum Graviton Decay into Muon Pairs", CMS NOTE-2006/104.

[7] I. Belotelov *et al.*, "Search for ADD Extra Dimensional Gravity in Dimuon Channel with the CMS Detector", CMS Note-2006/076.

[8] D. Bourilkov, "Sensitivity to contact interactions and extra dimensions in di-lepton and di-photon channels at future colliders," arXiv:hep-ph/0305125.

[9] D. Bourilkov, "Compositeness Search with Di-muons in CMS", CMS NOTE 2006/085.

[10] S. Haywood *et al.*, "Electroweak physics," arXiv:hep-ph/0003275.

[11] CMS Physics Generators Interface, http://cmsdoc.cern.ch/cmsoo/projects/CMKIN/index.html

[12] T. Sjöstrand, L. Lonnblad and S. Mrenna, [arXiv:hep-ph/0108264];
Pythia Home Page: http://www.thep.lu.se/tf2/staff/torbjorn/Pythia.html

[13] H.L. Lai *et al.* Eur. Phys. J. **C12** (2000) 375 [arXiv:hep-ph/9903282]

[14] CMS Coll., Object oriented Simulation for CMS Analysis and Reconstruction, Physics TDR Vol.I, Chapter 2, OSCAR home page: http://cmsdoc.cern.ch/OSCAR/

[15] CMS Coll., Object-oriented Reconstruction for CMS Analysis, Physics TDR Vol.I, Chapter 2, ORCA home page: http://cmsdoc.cern.ch/ORCA/

[16] The TriDAS Project, TDR, Vol.II : Data Acquisition and High-Level Trigger, Chapter 15, CERN/LHCC 02-26 CMS TDR 6 December 15, 2002.

[17] CMS Physics TDR, Vol.1, CERN-LHCC-2006-001, 2 February 2006.

[18] I. Belotelov et al., "Influence of Misalignment Scenarios on Muon reconstruction", CMS Note 2006/017;
I. Belotelov et al., "Simulation of Misalignment Scenarios for CMS Tracking Devices", CMS Note 2006/008.

[19] CMS Coll., FAMOS, FAst MOnte-Carlo Simulation, Physics TDR Vol.I, Section 2.6, FAMOS home page: http://cmsdoc.cern.ch/FAMOS/

[20] P. Langacker, R. W. Robinett and J. L. Rosner, Phys. Rev. D **30** (1984) 1470.

[21] M. Dittmar, A. S. Nicollerat and A. Djouadi, Phys. Lett. B **583** (2004) 111.

[22] R. Cousins, J. Mumford and V. Valuev, CMS NOTE 2005/022, CMS NOTE-2006/062 .

[23] M. Dittmar, F. Pauss and D. Zurcher, Phys. Rev. D **56** (1997) 7284 [arXiv:hep-ex/9705004].

[24] R. Hamberg, W. L. van Neerven and T. Matsuura, Nucl. Phys. B **359** (1991) 343 [Erratum-ibid. B **644** (2002) 403].

[25] U. Baur and D. Wackeroth, Nucl. Phys. Proc. Suppl. **116** (2003) 159 [arXiv:hep-ph/0211089].

[26] V. Zykunov, "Weak radiative corrections to the Drell-Yan process for large invariant mass of a dilepton pair", to be published in Phys. Rev. D [arXiv:hep-ph/0509315]

[27] M. R. Whalley, D. Bourilkov and R. C. Group, "The Les Houches accord PDFs (LHAPDF) and LHAGLUE," arXiv:hep-ph/0508110.

[28] D. Bourilkov, "Study of parton density function uncertainties with LHAPDF and PYTHIA at LHC," arXiv:hep-ph/0305126.

[29] http://durpdg.dur.ac.uk/lhapdf/

[30] J. Pumplin *et al.*, "New Generation of Parton Distributions with Uncertainties from Global QCD Analysis", JHEP 0207 (2002) 012, hep-ph/0201195.

[31] P. Bartalini, R. Chierici, A. De Roeck, "Guidelines for the Estimation of Theoretical Uncertainties at the LHC", CMS NOTE-2005/013.

[32] J. L. Rosner, Phys. Rev. D **35** (1987) 2244.

[33] M. Dittmar, Phys. Rev. D **55** (1997) 161.